Whirling Analysis of Stepped Timoshenko Shaft Carrying Several Rigid Disks

Ch. Kandouci[*]
Department of Maritime Engineering,
University of Sciences and Technology USTO-MB of Oran, Algeria
[*]*ch.kandouci@gmail.com*

ABSTRACT

Rotor system is the main part of turbomachines. Critical speeds occur when the rotor spin-speed matches with its natural frequencies, and result in great vibration amplitudes often leading to catastrophic failure. Design specifications based on these critical speeds become essential for the engineer. In this paper, whirling vibrations of a spinning, stepped Timoshenko shaft carrying three identical rigid disks are solved using a developed program in Fortran 90 language, based on relationships between the solution coefficient vectors of differential equations of motion. The flexural vibrations are considered in two orthogonal planes. Shear deformation, rotary inertia, and gyroscopic moments are taken into account. This study shows that in the case of the Timoshenko model, the relationship matrix form between the aforementioned vectors presents an advantage, that reduces the number of multiplied matrices when adjacent shaft segments have the same mechanical and geometric properties. The presented approach and Natanson's technique are combined to determine the whirling mode shapes. The accuracy of the presented technique is confirmed by comparing the obtained results with those available in the literature.

Keywords: *Timoshenko Shaft Segment; Vibration; Gyroscopic Effect; Vector of Solution Coefficients; Transfer Matrix*

Introduction

In the calculation of dynamic characteristics of spinning shaft-disk systems, the orthogonality hypothesis of the cross-section to the centerline after deformation, and the neglect of shear deformation, are justified for slender

ISSN 1823-5514, eISSN2550-164X
Received for review: 2021-08-29
© 2022 College of Engineering,
Universiti Teknologi MARA (UiTM), Malaysia.
Accepted for publication: 2022-02-28
Published: 2022-04-15

shafts, since it is well known that the effects of mentioned factors are small. However, the classical Bernoulli-Euler beam theory is also known to be imprecise for the vibration of higher modes, due to the induced mathematical modeling error, in the critical speed prediction. With the increasing demand for high-speed rotating machinery subjected to a wide range of speed changes, it has become necessary to discuss higher orders of vibration. Thus, the Timoshenko beam theory, which includes the rotary inertia and shear deformation of the cross-section, is applied in order to improve the accuracy of vibration analysis of the general rotating shaft. Additionally, the bending vibrations of rotating shafts are peculiarly characterized by gyroscopic moments.

Whirling vibration is a source of noise and fatigue failure of the rotating shaft [1]. Klanner et al. [2] presented a quasi-analytical solution for the whirling motion of multi-stepped rotors using the Rayleigh beam theory including rotary inertia and gyroscopic effects. Among studies based on the Timoshenko beam theory that focused on the whirling of rotors, Eshleman and Eubanks [3] investigated analytically the effect of axial torque on critical speeds of a uniform shaft taking into account the gyroscopic moment effect of the shaft. Bose and Sathujoda [4] studied the effects of variations in material gradation and thermal gradients on the whirl frequencies of a functionally graded rotor-bearing system, using the finite element method. Curti et al. [5] proposed an analytical method, based on the dynamic stiffness matrix of rotating-beam, for dynamic rotor analysis. Zu and Han [6] solved analytically the free bending vibrations of a spinning, finite beam for the six classical boundary conditions, and concluded that the simply-supported beam possesses two sets of natural frequencies corresponding to each mode shape, with identical forward and backward mode shapes, corresponding to each set. Han et al. [7] solved analytically the dynamics of a simply supported, spinning shaft subjected to a moving load, using the modal analysis method. Raffa and Vatta [8] studied the gyroscopic effects in the Lagrangian formulation of a rotating beam, by comparison of two Lagrangian densities differing from each other by the expression of gyroscopic terms. Hsieh et al. [9] developed a modified transfer matrix method to analyze the coupled lateral and torsional vibrations of a symmetric rotor-bearing with an external torque, and they determined the synchronous and superharmonic whirls in steady-state using the harmonic balance method. Raffa and Vatta [10] established the motion equations of an asymmetric shaft using the Lagrangian density formulation for continuous systems. Shiau et al. [11] analyzed the dynamic behavior of a spinning beam subjected to a moving skew force with general boundary conditions, using global assumed mode method. They deduced that the axial deflections due to the skew force are larger in the case of hinged-hinged boundary. Torabi and Afshari [12] analyzed the whirling of the rotor and investigated the effect of angular velocity of spin, axial load, slenderness, and Poisson's ratio on its forward and backward frequencies. Afshari et al. [13] analyzed the gyroscopic

effects on free transverse vibrations of multi-stepped rotors resting on bearings each replaced by four springs acting in two perpendicular directions, using the differential quadrature element method, and the Timoshenko beam theory. Y. Zhang et al. [14] developed a mathematical model of a rotating shaft with centrifugal terms using Hamilton's principle and Euler angles. They investigated the effect of centrifugal terms on the rotor stability by modal analysis. Afshari et al. [15] presented a solution using concepts of Dirac's delta function for whirling analysis of rotors carrying several concentrated masses. They showed the effect of point masses and the value of their translational inertia on vibration characteristics of rotors. Wu and Hsu [16] proposed an analytical approach for forward and backward whirling speeds and the associated mode shapes of uniform and nonuniform (stepped) shaft-disk systems. In [16], the obtained results are compared with those obtained from the conventional finite element method (FEM), however, the fourth and fifth forward whirling mode shapes, of the nonuniform (two-step) shaft-disk

Physical Model of Multi-step Timoshenko Shaft-disk System

Equations of motion

Figure 1, shows a multi-step Timoshenko shaft composed of n uniform shaft segments [denoted by (1), (2), …, (i), (i+1), …, (n-1), (n)] each with the corresponding length L_i, carrying several rigid disks each with a mass m_i, polar moment of inertia $J_{P,i}$, and diametric moment of inertia $J_{d,i}$.

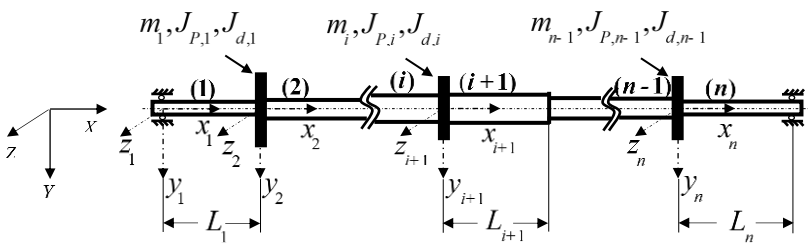

Figure 1: A nonuniform (multi-step) shaft carrying several rigid disks

The division is made at the junction of two adjacent shaft segments which have different mechanical and/or geometric properties, and at section passing through the center of gravity of disk (i) joining two shaft segments (i) and (i+1). The analyzed physical model is considered to be a linear system, and it is assumed that each disk (i) represents a discrete mass. For each shaft

segment (*i*), a fixed coordinate system $(x_i,\ y_i,\ z_i)$ is adopted, whose axes are, respectively, parallel to the axes of the fixed reference system (X, Y, Z).

Differential equations of motion for rotors are available in many forms in the open literature. The equations of motion of the (*i*-th) rotating shaft segment taking into account the effects of transverse shear, rotary inertia, and gyroscopic moments can be presented as [22].

$$\bar{k}_i S_i G_i \left(\frac{\partial^2 u_{y,i}(x,t)}{\partial x^2} - \frac{\partial \psi_{z,i}(x,t)}{\partial x} \right) = \rho_i S_i \frac{\partial^2 u_{y,i}(x,t)}{\partial t^2} \tag{1}$$

$$\bar{k}_i S_i G_i \left(\frac{\partial^2 u_{z,i}(x,t)}{\partial x^2} + \frac{\partial \psi_{y,i}(x,t)}{\partial x} \right) = \rho_i S_i \frac{\partial^2 u_{z,i}(x,t)}{\partial t^2} \tag{2}$$

$$\begin{aligned} &\rho_i I_{z,i} \frac{\partial^2 \psi_{z,i}(x,t)}{\partial t^2} - \rho_i I_{i,p}\ \Omega \frac{\partial \psi_{y,i}(x,t)}{\partial t} - \\ &\bar{k}_i G_i S_i \left(\frac{\partial u_{y,i}(x,t)}{\partial x} - \psi_{z,i}(x,t) \right) - E_i I_{z,i} \frac{\partial^2 \psi_{z,i}(x,t)}{\partial x^2} = 0 \end{aligned} \tag{3}$$

$$\begin{aligned} &\rho_i I_{y,i} \frac{\partial^2 \psi_{y,i}(x,t)}{\partial t^2} + \rho_i I_{i,p}\ \Omega \frac{\partial \psi_{z,i}(x,t)}{\partial t} + \\ &\bar{k}_i G_i S_i \left(\frac{\partial u_{z,i}(x,t)}{\partial x} + \psi_{y,i}(x,t) \right) - \rho_i I_{y,i} \frac{\partial^2 \psi_{y,i}(x,t)}{\partial t^2} = 0 \end{aligned} \tag{4}$$

where;

$$E_i \left(N/m^2 \right), G_i \left(N/m^2 \right), I_i = I_{i,z} = I_{y,i} \left(m^4 \right), I_{i,p} \left(m^4 \right), S_i (m^2), \rho_i \left(kg/m^3 \right)$$

are modulus of elasticity, shear modulus, a diametric moment of inertia, polar moment of inertia, cross-sectional area, and mass density of the *i*th shaft segment. $u_{y,i}(x,t)$, $u_{z,i}(x,t)$ and $\psi_{z,i}(x,t)$, $\psi_{y,i}(x,t)$ indicate components of transverse displacement and their corresponding bending angles, respectively. $\bar{k}_i$ is the shear correction factor.

An element (d*x*) of the *i*th Timoshenko shaft segment in its fixed space coordinates $(x_i,\ y_i,\ z_i)$ is shown in Figures 2 (a, b). The quantities $\frac{\partial u_{y,i}}{\partial x}$ and $\frac{\partial u_{z,i}}{\partial x}$ represent slopes of the elastic axis of the element, $\psi_{z,i}$ and $\psi_{y,i}$ denote

slopes due to bending, $\gamma_{xy,i}$ and $\gamma_{xz,i}$ are the shear angles between the elastic axis and the perpendicular to the shear face in (a) the xy -plane, and (b) the xz -plane.

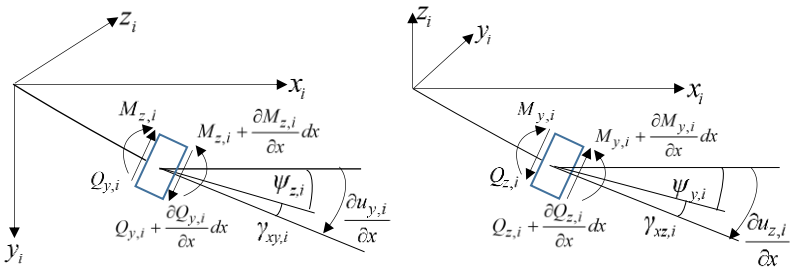

Figure 2: Element dx of i-th Timoshenko shaft segment: a- in (x_i y_i) plane, b- in (x_i z_i) plane

To avoid solving the coupled equations, the following complex variables have been introduced:

$$u_i(x,t) = u_{y,i}(x,t) + ju_{z,i}(x,t), \tag{5a}$$

$$\psi_i(x,t) = \psi_{z,i}(x,t) - j\psi_{y,i}(x,t), \tag{5b}$$

with $j = \sqrt{-1}$. Equations (1-4) are combined to obtain two complete partial differential equations of motion by multiplying Equations (2) and (4) by j and adding them to Equations (1) and (3), respectively. Equations (1-4) become:

$$\bar{k}_i S_i G_i \left(\frac{\partial^2 u_i(x,t)}{\partial x^2} - \frac{\partial \psi_i(x,t)}{\partial x} \right) = \rho_i S_i \frac{\partial^2 u_i(x,t)}{\partial t^2} \tag{6a}$$

$$\begin{aligned} &\rho_i I_i \frac{\partial^2 \psi_i(x,t)}{\partial t^2} - j\rho_i I_{i,p}\, \Omega \frac{\partial \psi_i(x,t)}{\partial t} - \\ &\bar{k}_i G_i S_i \left(\frac{\partial u_i(x,t)}{\partial x} - \psi_i(x,t) \right) - E_i I_i \frac{\partial^2 \psi_i(x,t)}{\partial x^2} = 0 \end{aligned} \tag{6b}$$

By differentiating Equations (6b) with respect to x, and taking into account (6a), the following equation can be obtained:

$$\rho_i S_i \frac{\partial^2 u_i(x,t)}{\partial t^2} = \rho_i I_i \frac{\partial^3 \psi_i(x,t)}{\partial x \partial t^2} - j\rho_i I_{i,p}\ \Omega \frac{\partial \psi_i(x,t)}{\partial x \partial t} - E_i I_i \frac{\partial^3 \psi_i(x,t)}{\partial x^3} = 0 \tag{7a}$$

The expression $\frac{\partial \psi_i(x,t)}{\partial x}$ can be derived from Equation (6a) as follows:

$$\frac{\partial \psi_i(x,t)}{\partial x} = \frac{\partial^2 u_i(x,t)}{\partial x^2} - \frac{\rho_i}{\bar{k}_i G_i} \frac{\partial^2 u_i(x,t)}{\partial t^2} \tag{7b}$$

Substituting the expression $\frac{\partial \psi_i(x,t)}{\partial x}$ given by Equation (7b) into Equation (7a) produces:

$$E_i I_i \frac{\partial^4 u_i(x,t)}{\partial x^4} - \rho_i I_i \left(1 + \frac{E_i}{\bar{k}_i G_i}\right) \frac{\partial^4 u_i(x,t)}{\partial t^2 \partial x^2} + \frac{\rho_i^2 I_i}{\bar{k}_i G_i} \frac{\partial^4 u_i(x,t)}{\partial t^4} + + j\rho_i I_{i,p} \Omega \left(\frac{\partial^3 u_i(x,t)}{\partial t \partial x^2} - \frac{\rho_i}{\bar{k}_i G_i} \frac{\partial^3 u_i(x,t)}{\partial t^3} \right) + \rho_i\ S_i \frac{\partial^2 u_i(x,t)}{\partial t^2} = 0 \tag{8a}$$

The expression for $\frac{\partial u_i(x,t)}{\partial x}$ can be derived from Equation (6b) as follows:

$$\frac{\partial u_i(x,t)}{\partial x} = \psi_i(x,t) + \frac{\rho_i I_i}{\bar{k}_i G_i S_i} \frac{\partial^2 \psi_i(x,t)}{\partial t^2} - j \frac{\rho_i I_{i,p}\ \Omega}{\bar{k}_i G_i S_i} \frac{\partial \psi_i(x,t)}{\partial t} - \frac{E_i I_i}{\bar{k}_i G_i S_i} \frac{\partial^2 \psi_i(x,t)}{\partial x^2} \tag{8b}$$

Differentiating Equation (7a) with respect to *x*, and substituting in it the expression of $\frac{\partial u_i(x,t)}{\partial x}$ given by Equation (8b), the following equation can be obtained:

$$E_i I_i \frac{\partial^4 \psi_i(x,t)}{\partial x^4} - \rho_i I_i \left(1 + \frac{E_i}{\bar{k}_i G_i}\right) \frac{\partial^4 \psi_i(x,t)}{\partial t^2 \partial x^2} + \frac{\rho_i^2 I_i}{\bar{k}_i G_i} \frac{\partial^4 \psi_i(x,t)}{\partial t^4} + j\rho_i I_{i,p} \Omega \left(\frac{\partial^3 \psi_i(x,t)}{\partial t \partial x^2} - \frac{\rho_i}{\bar{k}_i G_i} \frac{\partial^3 \psi_i(x,t)}{\partial t^3} \right) + \rho_i\ S_i \frac{\partial^2 \psi_i(x,t)}{\partial t^2} = 0 \tag{9a}$$

Equations (8a) and (9a) represent the uncoupled equations of motion. The complex variable representation of the shear angle is:

$$\gamma_i(x,t) = \left(\frac{\partial u_i(x,t)}{\partial x} - \psi_i(x,t) \right) \tag{9b}$$

The vibrational solutions of Equations (8a) and (9a) can be written as:

$$u_i(x,t) = \bar{u}_i(x)\, e^{\pm j\omega t} \tag{10a}$$

$$\psi_i(x,t) = \bar{\psi}_i(x)\, e^{\pm j\omega t} \tag{10b}$$

where $\bar{u}_i(x)$ and $\bar{\psi}_i(x)$ are the shape functions of $u_i(x,t)$ and $\psi_i(x,t)$, respectively, ω the whirling frequency of the Timoshenko shaft-disk system. The upper sign $(+)$ and lower sign $(-)$ refer to forward and backward whirls, respectively. Substituting Equations (10a, b) into Equations (8a) and (9a) results in the following equations:

$$\frac{d^4\bar{u}_i(x)}{dx^4} + (r_1 + r_2)\frac{d^2\bar{u}_i(x)}{dx^2} - (r_3 - r_1 r_2)\bar{u}_i(x) = 0 \tag{11}$$

$$\frac{d^4\bar{\psi}_i(x)}{dx^4} + (r_1 + r_2)\frac{d^2\bar{\psi}_i(x)}{dx^2} - (r_3 - r_1 r_2)\bar{\psi}_i(x) = 0 \tag{12}$$

where;

$$r_1 = \frac{\rho_i \omega^2}{\bar{k}_i G_i}, \quad r_2 = \frac{(\rho_i I_i \omega^2 \pm \rho_i I_{i,p} \Omega\omega)}{E_i I_i}, \quad r_3 = \frac{\rho_i S_i \omega^2}{E_i I_i} \tag{13}$$

The solutions to Equations (11) and (12) are:

$$\bar{u}_i(x) = a_{i1}\sin\lambda_1^{(i)}x + a_{i2}\cos\lambda_1^{(i)}x + a_{i3}\sinh\lambda_2^{(i)}x + a_{i4}\cosh\lambda_2^{(i)}x \tag{14}$$

$$\bar{\psi}_i(x) = \tilde{a}_{i1}\sin\lambda_1^{(i)}x + \tilde{a}_{i2}\cos\lambda_1^{(i)}x + \tilde{a}_{i3}\sinh\lambda_2^{(i)}x + \tilde{a}_{i4}\cosh\lambda_2^{(i)}x \tag{15}$$

where:

$$\lambda_1^{(i)} = \left\{ \frac{1}{2}\left[4(r_3 - r_1 r_2) + (r_1 + r_2)^2 \right]^{\frac{1}{2}} + \frac{1}{2}(r_1 + r_2) \right\}^{\frac{1}{2}} \tag{16}$$

$$\lambda_2^{(i)} = \left\{ \frac{1}{2}\left[4(r_3 - r_1 r_2) + (r_1 + r_2)^2 \right]^{\frac{1}{2}} - \frac{1}{2}(r_1 + r_2) \right\}^{\frac{1}{2}} \tag{17}$$

Substituting Equations (10a,b) into Equation (6a), yields:

$$\tilde{a}_{i1} = -\beta_1^{(i)} a_{i2}, \quad \tilde{a}_{i2} = \beta_1^{(i)} a_{i1}, \quad \tilde{a}_{i3} = \beta_2^{(i)} a_{i4}, \quad \tilde{a}_{i4} = \beta_2^{(i)} a_{i3} \tag{18}$$

The Equations (14) and (15) can be rewritten as follows:

$$\bar{u}_i(x) = a_{i1} \sin\lambda_1^{(i)} x + a_{i2} \cos\lambda_1^{(i)} x + a_{i3} \sinh\lambda_2^{(i)} x + a_{i4} \cosh\lambda_2^{(i)} x \tag{19}$$

$$\bar{\psi}_i(x) = a_{i1}\beta_1^{(i)} \cos\lambda_1^{(i)} x - a_{i2}\beta_1^{(i)} \sin\lambda_1^{(i)} x + a_{i3}\beta_2^{(i)} \cosh\lambda_2^{(i)} x + a_{i4}\beta_2^{(i)} \sinh\lambda_2^{(i)} x \tag{20}$$

Taking $w_i = \{u_i, \psi_i\}$ as vibration vector, this will produce:

$$w_i = \bar{w}_i(x)\, e^{\pm j\omega t} \tag{21}$$

$$\bar{w}_i(x) = A_i(x)\, V_i \tag{22}$$

where:

$$A_i(x) = \begin{bmatrix} \sin\lambda_1^{(i)} x & \cos\lambda_1^{(i)} x & \sinh\lambda_2^{(i)} x & \cosh\lambda_2^{(i)} x \\ \beta_1^{(i)} \cos\lambda_1^{(i)} x & -\beta_1^{(i)} \sin\lambda_1^{(i)} x & \beta_2^{(i)} \cosh\lambda_2^{(i)} x & \beta_2^{(i)} \sinh\lambda_2^{(i)} x \end{bmatrix}$$

and V_i is the vector column of solution coefficients for the i-th shaft segment.

$$V_i = \left[a_{i1},\ a_{i2},\ a_{i3},\ a_{i4} \right]^T \tag{23}$$

According to the Timoshenko beam theory, components of bending moment and shear force are [22]:

$$M_{z,i}(x,t) = E_i I_i \frac{\partial \psi_{z,i}(x,t)}{\partial x}, \quad M_{y,i}(x,t) = E_i I_i \frac{\partial \psi_{y,i}(x,t)}{\partial x} \tag{24a}$$

$$Q_{y,i}(x,t) = \bar{k}_i G_i S_i \gamma_{xy,i}(x,t), \quad Q_{z,i}(x,t) = -\bar{k}_i G_i S_i \gamma_{xz,i}(x,t) \tag{24b}$$

where;

$$\gamma_{xy,i}(x,t) = \frac{\partial u_{y,i}(x,t)}{\partial x} - \psi_{z,i}(x,t), \quad \gamma_{xz,i}(x,t) = \frac{\partial u_{z,i}(x,t)}{\partial x} + \psi_{y,i}(x,t) \tag{25}$$

$\gamma_i(x,t) = \gamma_{xy,i}(x,t) + j\gamma_{xz,i}(x,t)$ is the complex representation of shear angle. Taking into account Equations (10a,b), real parts of bending moments and shear forces can be written as:

$$\bar{M}_{z,i}(x) = E_i I_i \frac{\partial \bar{\psi}_{z,i}(x)}{\partial x}, \quad \bar{M}_{y,i}(x) = E_i I_i \frac{\partial \bar{\psi}_{y,i}(x)}{\partial x} \tag{26a}$$

$$\bar{Q}_{y,i}(x) = \bar{k}_i G_i S_i \bar{\gamma}_{xy,i}(x), \quad \bar{Q}_{z,i}(x) = -\bar{k}_i G_i S_i \bar{\gamma}_{xz,i}(x) \tag{26b}$$

If external damping due to the hydrodynamic bearing effect is not included, the boundary conditions at the left and right ends of the system depicted in Figure 1, can be considered as:

$$\bar{u}_{y,1}(0) = 0, \quad \bar{u}_{z,1}(0) = 0, \quad E_1 I_1 \bar{\psi}'_{z,1}(0) = 0, \quad E_1 I_1 \bar{\psi}'_{y,1}(0) = 0 \tag{27a}$$

$$\bar{u}_{y,n}(L_n) = 0, \quad \bar{u}_{z,n}(L_n) = 0, \quad E_n I_n \bar{\psi}'_{z,n}(L_n) = 0, \quad E_n I_n \bar{\psi}'_{y,n}(L_n) = 0 \tag{27b}$$

In terms of the complex numbers, the preceding Equations (27a,b) are reduced to the following relations:

$$\bar{u}_1(0) = 0, \qquad E_1 I_1 \bar{\psi}'_1(0) = 0 \tag{28a}$$

$$\bar{u}_n(L_n) = 0, \qquad E_n I_n \bar{\psi}'_n(L_n) = 0 \tag{28b}$$

Vectors of solution coefficients

A junction of two adjacent shaft segments is depicted in Figure 3. L_i is the length of the *i*th shaft segment,

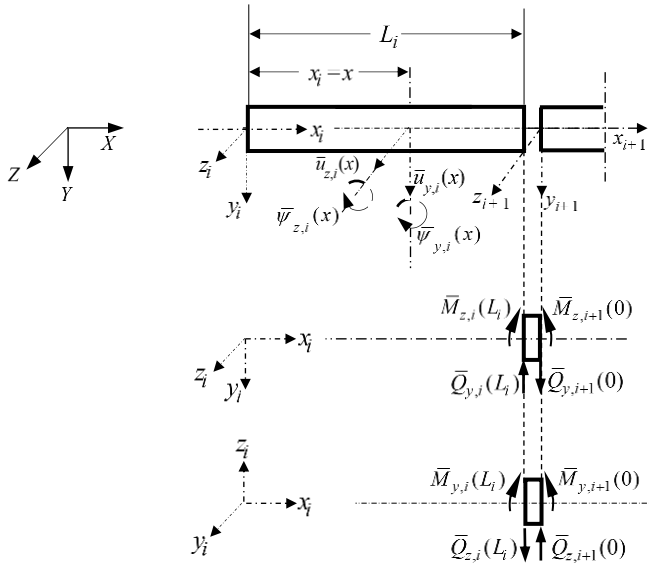

Figure 3: Shear forces and bending moments acting at the junction of two adjacent shaft segments (i) and $(i+1)$

Case of shaft segments with different mechanical and/or geometric properties

At the junction joining two shaft segments having different mechanical and/or geometric properties, the equations for continuity of displacements and bending slopes are given by:

$$\bar{u}_{y,i}(L_i) = \bar{u}_{y,i+1}(0) \tag{29a}$$

$$\bar{u}_{z,i}(L_i) = \bar{u}_{z,i+1}(0) \tag{29b}$$

$$\bar{\psi}_{z,i}(L_i) = \bar{\psi}_{z,i+1}(0) \tag{30a}$$

$$\bar{\psi}_{y,i}(L_i) = \bar{\psi}_{y,i+1}(0) \tag{30b}$$

Taking into account Equations (5a) and (5b), Equations (29a,b) and (30a,b) become:

$$\bar{u}_i(L_i) = \bar{u}_{i+1}(0) \tag{31}$$

$$\bar{\psi}_i(L_i) = \bar{\psi}_{i+1}(0) \tag{32}$$

Equations (31) and (32) can be expressed in a vector form as follows:

$$\bar{w}_i(L_i) = \bar{w}_{i+1}(0) \tag{33}$$

Thus:

$$A_i(L_i)\ V_i = A_{i+1}(0)\ V_{i+1} \tag{34}$$

where:

$$A_i(L_i) = \begin{bmatrix} \sin\lambda_1^{(i)}L_i & \cos\lambda_1^{(i)}L_i & \sinh\lambda_2^{(i)}L_i & \cosh\lambda_2^{(i)}L_i \\ \beta_1^{(i)}\cos\lambda_1^{(i)}L_i & -\beta_1^{(i)}\sin\lambda_1^{(i)}L_i & \beta_2^{(i)}\cosh\lambda_2^{(i)}L_i & \beta_2^{(i)}\sinh\lambda_2^{(i)}L_i \end{bmatrix}$$

$$A_{i+1}(0) = \begin{bmatrix} 0 & 1 & 0 & 1 \\ \beta_1^{(i+1)} & 0 & \beta_2^{(i+1)} & 0 \end{bmatrix}$$

The equilibrium equations for shear forces and bending moments require that:

$$\bar{M}_{z,i}(L_i) = \bar{M}_{z,i+1}(0) \tag{35a}$$

$$\bar{M}_{y,i}(L_i) = \bar{M}_{y,i+1}(0) \tag{35b}$$

$$\bar{Q}_{y,i}(L_i) = \bar{Q}_{y,i+1}(0) \tag{36a}$$

$$\bar{Q}_{z,i}(L_i) = \bar{Q}_{z,i+1}(0) \tag{36b}$$

Taking into account relationships (26a,b), the equilibrium Equations (35a,b) and (36a,b) become:

$$E_i I_i \bar{\psi}'_{z,i}(L_i) = E_{i+1} I_{i+1} \bar{\psi}'_{z,i+1}(0) \tag{37a}$$

$$E_i I_i \bar{\psi}'_{y,i}(L_i) = E_{i+1} I_{i+1} \bar{\psi}'_{y,i+1}(0) \tag{37b}$$

$$\bar{k}_i G_i S_i\ \bar{\gamma}_{xy,i}(L_i) = \bar{k}_{i+1} G_{i+1} S_{i+1}\ \bar{\gamma}_{xy,i+1}(0) \tag{38a}$$

$$-\bar{k}_i G_i S_i\ \bar{\gamma}_{xz,i}(L_i) = -\bar{k}_{i+1} G_{i+1} S_{i+1}\ \bar{\gamma}_{xz,i+1}(0) \tag{38b}$$

Equations (37a,b) and (38a,b) can be derived in terms of the following complex numbers:

$$E_i I_i \bar{\psi}_i'(L_i) = E_{i+1} I_{i+1} \bar{\psi}_{i+1}'(0) \tag{39}$$

$$\bar{k}_i G_i S_i \ \bar{\gamma}_i(L_i) = \bar{k}_{i+1} G_{i+1} S_{i+1} \ \bar{\gamma}_{i+1}(0) \tag{40}$$

Hence, we get the following matrix form:

$$D_i(L_i)\ V_i = D_{i+1}(0)\ V_{i+1} \tag{41}$$

where;

$$D_i(L_i) = \begin{bmatrix} \Gamma_1 & \mathrm{M}\ \Gamma_2 \end{bmatrix}$$

$$\Gamma_1 = \begin{bmatrix} -E_i I_i \lambda_1^{(i)} \beta_1^{(i)} \sin \lambda_1^{(i)} L_i & -E_i I_i \lambda_1^{(i)} \beta_1^{(i)} \cos \lambda_1^{(i)} L_i \\ \bar{k}_i G_i S_i (\lambda_1^{(i)} \cos \lambda_1^{(i)} L_i - \beta_1^{(i)} \cos \lambda_1^{(i)} L_i) & \bar{k}_i G_i S_i (-\lambda_1^{(i)} \sin \lambda_1^{(i)} L_i + \beta_1^{(i)} \sin \lambda_1^{(i)} L_i) \end{bmatrix}$$

$$\Gamma_2 = \begin{bmatrix} E_i I_i \lambda_2^{(i)} \beta_2^{(i)} \sinh \lambda_2^{(i)} L_i & E_i I_i \lambda_2^{(i)} \beta_2^{(i)} \cosh \lambda_2^{(i)} L_i \\ \bar{k}_i G_i S_i (\lambda_2^{(i)} \cosh \lambda_2^{(i)} L_i - \beta_2^{(i)} \cosh \lambda_2^{(i)} L_i) & \bar{k}_i G_i S_i (\lambda_2^{(i)} \sinh \lambda_2^{(i)} L_i - \beta_2^{(i)} \sinh \lambda_2^{(i)} L_i) \end{bmatrix}$$

$D_{i+1}(0)=$

$$\begin{bmatrix} 0 & -E_{i+1} I_{i+1} \lambda_1^{(i+1)} \beta_1^{(i+1)} & 0 & E_{i+1} I_{i+1} \lambda_2^{(i+1)} \beta_2^{(i+1)} \\ \bar{k}_{i+1} G_{i+1} S_{i+1} (\lambda_1^{(i+1)} - \beta_1^{(i+1)}) & 0 & \bar{k}_{i+1} G_{i+1} S_{i+1} (\lambda_2^{(i+1)} - \beta_2^{(i+1)}) & 0 \end{bmatrix}$$

Finally, the following relationship can be obtained:

$$V_{i+1} = B_i\ V_i \tag{42}$$

with:

$$B_i = \begin{bmatrix} A_{i+1}(0) \\ D_{i+1}(0) \end{bmatrix}^{-1} \begin{bmatrix} A_i(L_i) \\ D_i(L_i) \end{bmatrix} \tag{43}$$

The matrix B_i can be called a transfer matrix related to the vectors of solution coefficients. It has the following form:

$$B_i = \begin{bmatrix} -\mu_1 \cos(\lambda_1^{(i)} L_i) & \mu_1 \sin(\lambda_1^{(i)} L_i) & \mu_2 \cosh(\lambda_2^{(i)} L_i) & \mu_2 \sinh(\lambda_2^{(i)} L_i) \\ \mu_3 \sin(\lambda_1^{(i)} L_i) & \mu_3 \cos(\lambda_1^{(i)} L_i) & \mu_4 \sinh(\lambda_2^{(i)} L_i) & \mu_4 \cosh(\lambda_2^{(i)} L_i) \\ -\mu_5 \cos(\lambda_1^{(i)} L_i) & \mu_5 \sin(\lambda_1^{(i)} L_i) & \mu_6 \cosh(\lambda_2^{(i)} L_i) & \mu_6 \sinh(\lambda_2^{(i)} L_i) \\ \mu_7 \sin(\lambda_1^{(i)} L_i) & \mu_7 \cos(\lambda_1^{(i)} L_i) & \mu_8 \sinh(\lambda_2^{(i)} L_i) & \mu_8 \cosh(\lambda_2^{(i)} L_i) \end{bmatrix} \tag{44}$$

with,

$$\mu_1 = \frac{(\beta_1^{(i)}\lambda_2^{(i+1)} - \beta_1^{(i)}\beta_2^{(i+1)})}{(\beta_2^{(i+1)}\lambda_1^{(i+1)} - \beta_1^{(i+1)}\lambda_2^{(i+1)})} + \frac{(\beta_1^{(i)}\beta_2^{(i+1)} - \beta_2^{(i+1)}\lambda_1^{(i)})}{(\beta_2^{(i+1)}\lambda_1^{(i+1)} - \beta_1^{(i+1)}\lambda_2^{(i+1)})} \frac{\bar{k}_i G_i S_i}{\bar{k}_{i+1} G_{i+1} S_{i+1}}$$

$$\mu_2 = \frac{(\beta_2^{(i+1)}\beta_2^{(i)} - \beta_2^{(i)}\lambda_2^{(i+1)})}{(\beta_2^{(i+1)}\lambda_1^{(i+1)} - \beta_1^{(i+1)}\lambda_2^{(i+1)})} + \frac{(\beta_2^{(i+1)}\lambda_2^{(i)} - \beta_2^{(i+1)}\beta_2^{(i)})}{\beta_2^{(i+1)}\lambda_1^{(i+1)} - \beta_1^{(i+1)}\lambda_2^{(i+1)}} \frac{\bar{k}_i G_i S_i}{\bar{k}_{i+1} G_{i+1} S_{i+1}}$$

$$\mu_3 = \frac{\beta_2^{(i+1)}\lambda_2^{(i+1)}}{(\beta_2^{(i+1)}\lambda_2^{(i+1)} + \beta_1^{(i+1)}\lambda_1^{(i+1)})} + \frac{\beta_1^{(i)}\lambda_1^{(i)}}{(\beta_2^{(i+1)}\lambda_2^{(i+1)} + \beta_1^{(i+1)}\lambda_1^{(i+1)})} \frac{E_i I_i}{E_{i+1} I_{i+1}}$$

$$\mu_4 = \frac{\beta_2^{(i+1)}\lambda_2^{(i+1)}}{(\beta_2^{(i+1)}\lambda_2^{(i+1)} + \beta_1^{(i+1)}\lambda_1^{(i+1)})} - \frac{\beta_2^{(i)}\lambda_2^{(i)}}{(\beta_2^{(i+1)}\lambda_2^{(i+1)} + \beta_1^{(i+1)}\lambda_1^{(i+1)})} \frac{E_i I_i}{E_{i+1} I_{i+1}}$$

$$\mu_5 = \frac{(\beta_1^{(i+1)}\beta_1^{(i)} - \beta_1^{(i)}\lambda_1^{(i+1)})}{(\beta_2^{(i+1)}\lambda_1^{(i+1)} - \beta_1^{(i+1)}\lambda_2^{(i+1)})} + \frac{(\beta_1^{(i+1)}\lambda_1^{(i)} - \beta_1^{(i+1)}\beta_1^{(i)})}{\beta_2^{(i+1)}\lambda_1^{(i+1)} - \beta_1^{(i+1)}\lambda_2^{(i+1)}} \frac{\bar{k}_i G_i S_i}{\bar{k}_{i+1} G_{i+1} S_{i+1}}$$

$$\mu_6 = \frac{(\beta_2^{(i)}\lambda_1^{(i+1)} - \beta_1^{(i+1)}\beta_2^{(i)})}{(\beta_2^{(i+1)}\lambda_1^{(i+1)} - \beta_1^{(i+1)}\lambda_2^{(i+1)})} - \frac{(\beta_1^{(i+1)}\lambda_2^{(i)} - \beta_1^{(i+1)}\beta_2^{(i)})}{\beta_2^{(i+1)}\lambda_1^{(i+1)} - \beta_1^{(i+1)}\lambda_2^{(i+1)}} \frac{\bar{k}_i G_i S_i}{\bar{k}_{i+1} G_{i+1} S_{i+1}}$$

$$\mu_7 = \frac{\beta_1^{(i+1)}\lambda_1^{(i+1)}}{(\beta_1^{(i+1)}\lambda_1^{(i+1)} + \beta_2^{(i+1)}\lambda_2^{(i+1)})} - \frac{E_i I_i}{E_{i+1} I_{i+1}} \frac{\beta_1^{(i)}\lambda_1^{(i)}}{(\beta_1^{(i+1)}\lambda_1^{(i+1)}\beta_2^{(i+1)}\lambda_2^{(i+1)})}$$

$$\mu_8 = \frac{\beta_1^{(i+1)}\lambda_1^{(i+1)}}{(\beta_1^{(i+1)}\lambda_1^{(i+1)} + \beta_2^{(i+1)}\lambda_2^{(i+1)})} + \frac{E_i I_i}{E_{i+1} I_{i+1}} \frac{\beta_2^{(i)}\lambda_2^{(i)}}{(\beta_1^{(i+1)}\lambda_1^{(i+1)} + \beta_2^{(i+1)}\lambda_2^{(i+1)})} \tag{45}$$

For shaft segments having the same mechanical and geometric properties, we get:

$$\frac{\bar{k}_i G_i S_i}{\bar{k}_{i+1} G_{i+1} S_{i+1}} = 1, \quad \frac{E_i I_i}{E_{i+1} I_{i+1}} = 1, \quad \lambda_1^{(i)} = \lambda_1^{(i+1)}$$
$$\lambda_2^{(i)} = \lambda_2^{(i+1)}, \quad \beta_1^{(i)} = \beta_1^{(i+1)}, \quad \beta_2^{(i)} = \beta_2^{(i+1)} \tag{46a}$$

i.e. the coefficients $\mu_1, \mu_2, ..., \mu_8$ reduce to:

$$\mu_1 = -1, \quad \mu_2 = \mu_4 = \mu_5 = \mu_7 = 0, \quad \mu_3 = \mu_6 = \mu_8 = 1 \tag{46b}$$

and then the matrix B_i takes the following block diagonal form:

$$B_i = \begin{bmatrix} \cos(\lambda_1^{(i)} L_i) & -\sin(\lambda_1^{(i)} L_i) & 0 & 0 \\ \sin(\lambda_1^{(i)} L_i) & \cos(\lambda_1^{(i)} L_i) & 0 & 0 \\ 0 & 0 & \cosh(\lambda_2^{(i)} L_i) & \sinh(\lambda_2^{(i)} L_i) \\ 0 & 0 & \sinh(\lambda_2^{(i)} L_i) & \cosh(\lambda_2^{(i)} L_i) \end{bmatrix} \quad (47)$$

The relationships between the following $(r-1)$ shaft segments can be expressed as:

$$V_{i+r} = B_{i+r-1} B_{i+r-2} .... B_i V_i \quad (48)$$

From Equation (47), it is easy to notice that in the case of shaft segments having the same physical and geometric properties, Equation (48) reduces to:

$$V_{i+r} = R_i \; V_i \quad (49)$$

where R_i is the matrix B_i from equation (47), with L_i replaced by:

$$L_i = \sum_{\nu=i}^{\nu=i+r-1} L_\nu \quad (50)$$

(The multiplication of this type of matrices can be replaced by argument summation of functions present in these matrices). This advantage does not exist with the well-known transfer matrices related to the state vectors. The presented approach keeps this advantage even if the linear model of internal damping is taken into account.

Case of adjacent shaft segments (*i*) and (*i*+1) joined by a discrete mass m_i

Figures 4 (a,b) show a discrete mass m_i with inertia matrix M_i, joining two adjacent shaft segments (*i*) and (*i*+1), rotating with spin speed Ω, on the vertical and horizontal planes, respectively. The approximate values of the angular speed components are given by:

$$\Omega_y = \Omega \sin \psi_{z,i}(L_i, t) \approx \Omega \; \psi_{z,i}(L_i, t) \quad (51a)$$

$$\Omega_z = \Omega \sin(-\psi_{y,i}(L_i, t)) \approx -\Omega \psi_{y,i}(L_i, t) \quad (51b)$$

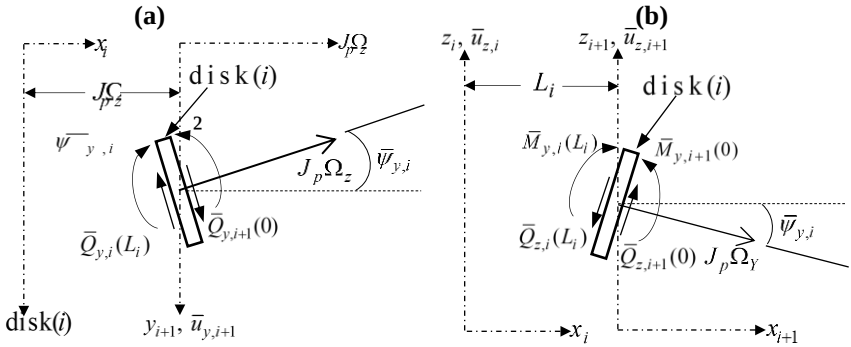

Figure 4: Forces and moments acting on rigid disk (*i*), joining two Timoshenko shaft segments (*i*) and (*i*+1), on (a) the *xy* - plane, and (b) the *xz* - plane

The center of gravity of each disk (*i*) and centroid of the cross-section of the shaft segment are assumed to coincide. If displacements are small, the following conditions of displacement continuity are verified:

$$\bar{u}_{y,i}(L_i) = \bar{u}_{y,i+1}(0) \tag{52a}$$

$$\bar{u}_{z,i}(L_i) = \bar{u}_{z,i+1}(0) \tag{52b}$$

$$\bar{\psi}_{z,i}(L_i) = \bar{\psi}_{z,i+1}(0) \tag{53a}$$

$$\bar{\psi}_{y,i}(L_i) = \bar{\psi}_{y,i+1}(0) \tag{53a}$$

Taking into account Equations (5a,b), (21) and (22), Equations (52a,b) and (53a,b) become:

$$\bar{u}_i(L_i) = \bar{u}_{i+1}(0) \tag{54a}$$

$$\bar{\psi}_i(L_i) = \bar{\psi}_{i+1}(0) \tag{54b}$$

$$\bar{w}_i(L_i) = \bar{w}_{i+1}(0) \tag{55a}$$

$$A_i(L_i)V_i = A_{i+1}(0)V_{i+1} \tag{55b}$$

The equilibrium equations at the disk (i) for shear forces and bending moments are:

$$Q_{y,i}(L_i,t) = Q_{y,i+1}(0,t) - m_i \frac{\partial^2 u_{y,i}(L_i,t)}{\partial t^2} \tag{56a}$$

$$Q_{z,i}(L_i,t) = Q_{z,i+1}(0,t) - m_i \frac{\partial^2 u_{z,i}(L_i,t)}{\partial t^2} \tag{56b}$$

$$M_{z,i}(L_i,t) = M_{z,i+1}(0,t) - J_{d,i} \frac{\partial^2 \psi_{z,i}(L_i,t)}{\partial t^2} - J_{p,i} \frac{\partial \Omega_z}{\partial t} \tag{57a}$$

$$M_{y,i}(L_i,t) = M_{y,i+1}(0,t) - J_{d,i} \frac{\partial^2 \psi_{y,i}(L_i,t)}{\partial t^2} - J_{p,i} \frac{\partial \Omega_y}{\partial t} \tag{57b}$$

where $J_{d,i}$ and $J_{p,i}$ are diametric and polar mass moments of inertia of the disk (i), respectively. Taking into account Equations (24b) and (26b), Equations (56a,b) become:

$$\bar{k}G_i S_i \bar{\gamma}_{xy,i}(L_i) - \omega^2 m_i \bar{u}_{y,i}(L_i) = \bar{k}G_{i+1} S_{i+1} \bar{\gamma}_{xy,i+1}(0) \tag{58a}$$

$$-\bar{k}G_i S_i \bar{\gamma}_{xz,i}(L_i) - \omega^2 m_i \bar{u}_{z,i}(L_i) = -\bar{k}G_{i+1} S_{i+1} \bar{\gamma}_{xz,i+1}(0) \tag{58b}$$

Substituting Equations (51a,b) and into Equations (57a,b), respectively, and taking into account Equations(24a), (26a), we get:

$$\left(EI_z\right)_i \bar{\psi}'_{z,i}(L_i) - \omega^2 J_{d,i} \bar{\psi}_{z,i}(L_i) - jJ_{p,i}\Omega\omega\bar{\psi}_{y,i}(L_i) = \left(EI_z\right)_{i+1} \bar{\psi}'_{z,i+1}(0) \tag{59a}$$

$$\left(EI_y\right)_i \bar{\psi}'_{y,i}(L_i) - \omega^2 J_{d,i} \bar{\psi}_{y,i}(L_i) + jJ_{P,i}\Omega\omega\bar{\psi}_{z,i}(L_i) = \left(EI_y\right)_{i+1} \bar{\psi}'_{y,i+1}(0) \tag{59b}$$

Multiplying Equation (58b) by j and adding it to Equation (58a), will produce:

$$\bar{k}G_i S_i \bar{\gamma}_i(L_i) - \omega^2 m_i \ \bar{u}_i(L_i) = \bar{k}G_{i+1} S_{i+1} \bar{\gamma}_{i+1}(0) \tag{60a}$$

Multiplying Equation (59b) by $(-j)$ and adding it to Equation (59a), we get:

$$\left(EI\right)_i \bar{\psi}'_i(L_i) - \omega^2 J_{d,i} \ \bar{\psi}_i(L_i) - J_{p,i} \ \Omega\omega\bar{\psi}_i(L_i) = \left(EI\right)_{i+1} \bar{\psi}'_{i+1}(0) \tag{60b}$$

Equations (60a,b) can be written in the following matrix form:

$$D_i(L_i)\ V_i - \omega^2 M_i A_i(L_i)\ V_i - J_{p,i}\ \Omega\ \omega\ \chi_i(L_i) V_i = D_{i+1}(0)\ V_{i+1} \tag{61}$$

where:

$$M_i = \begin{bmatrix} m_i & 0 \\ 0 & J_i \end{bmatrix}$$

and,

$$\chi_i(L_i) = \begin{bmatrix} 0 & 0 & 0 & 0 \\ \beta_1^{(i)} \cos \lambda_1^{(i)} L_i & -\beta_1^{(i)} \sin \lambda_1^{(i)} L_i & \beta_2^{(i)} \cosh \lambda_2^{(i)} L_i & \beta_2^{(i)} \sinh \lambda_2^{(i)} L_i \end{bmatrix}$$

while,

$$V_i = \left[a_{i1},\ a_{i2},\ a_{i3},\ a_{i4}\right]^T \tag{62}$$

Equations (55b) and (61), can be expressed in the following matrix form:

$$V_{i+1} = H_i\ V_i \tag{63}$$

where,

$$H_i = \begin{bmatrix} A_{i+1}(0) \\ D_{i+1}(0) \end{bmatrix}^{-1} \begin{bmatrix} A_i(L_i) \\ D_i(L_i) - \omega^2 M_i A_i(L_i) + \ \Omega\ \omega J_{p,i}\ \chi_i(L_i) \end{bmatrix} \tag{64}$$

H_i represents the transfer matrix related to the vector of solution coefficients V_i, through the disk (i) taking into account its gyroscopic effect. The vectors of solution coefficients V_2, V_3,...,V_n, can be determined by means of the above-derived transfer matrices, as followed:

$$\begin{aligned} &V_2 = B_1 V_1, \\ &V_3 = B_2\ a_2 = B_2 B_1 V_1 \\ &V_4 = H_3\ a_3 = B_3 B_2 B_1 V_1 \\ &\vdots \\ &V_n = B_{n-1} B_{n-2} \ldots B_3 B_2 B_1 V_1. \end{aligned} \tag{65}$$

Natural frequencies, whirling speeds, and mode shapes

Derived in terms of complex variables, the boundary conditions become:

$$\bar{u}_1(0)=0,\ E_1I_1\bar{\psi}_1'(0)=0,\quad \bar{u}_n(L_n)=0,\ E_nI_n\bar{\psi}_n'(L_n)=0 \tag{66}$$

Finally, the boundary conditions (66) can be written, respectively, as:

$$\Pi_1(0)\ V_1=0,\qquad \Pi_n(L_n)\ V_n=0 \tag{67}$$

Using the relationships (65), the boundary conditions can be written in the following matrix form:

$$\begin{bmatrix} \Pi_1(0) \\ \Pi_n(L_n)B_{n-1}...B_3B_2B_1 \end{bmatrix}\{V_1\}=0 \tag{68}$$

thus, the boundary conditions are expressed as a function of V_1, which is the constant coefficient column vector for whirling vibrations of the first Timochenko shaft segment (i=1).

$$V_1=\left[a_{11},\ a_{12},\ a_{13},\ a_{14}\right]^T \tag{69}$$

According to Equations (65), the column vector V_1 verifies the following equation:

$$C_1V_1=0 \tag{70}$$

where,

$$C_1=\begin{pmatrix} \alpha_{11} & \mathrm{K} & \alpha_{14} \\ \mathrm{M} & \mathrm{O} & \mathrm{M} \\ \alpha_{41} & \mathrm{L} & \alpha_{44} \end{pmatrix}=\begin{bmatrix} \Pi_1(0) \\ \Pi_n(L_n)B_{n-1}\ ...\ B_3B_2B_1 \end{bmatrix} \tag{71}$$

Equation (70) represents the characteristic equation. Nontrivial solution for the column vector V_1, requires that:

$$\left|C_1\right|=0 \tag{72}$$

The above expression is an eigenvalue equation. Natural frequencies (ω_s) of the non-rotating system and critical whirling speeds ($\widetilde{\omega}_s$) may be obtained by solving the eigenvalue Equation (72), for ($\Omega=0$) and ($\Omega=\widetilde{\omega}_s$), using the modified half-interval method [23].

According to Natanson [21], in the case of a singular matrix, the column vector V_1 in Equation (70) can be estimated up to a multiplicative constant ϕ, as follow:

$$a_{11} = \phi f_{11}, \quad a_{12} = \phi f_{12}, \quad a_{13} = \phi f_{13}, \quad a_{14} = \phi f_{14} \tag{73}$$

where $f_{1\alpha}(\alpha = 1,...,4)$ denote the algebraic complements of corresponding elements $\alpha_{1\nu}(\nu = 1,...,4)$ of the matrix C_1. The vibration mode shape of the first shaft segment (i=1) can be expressed as:

$$\bar{u}_1(x) = g_{11} \sin \lambda_1^{(1)} x + g_{12} \cos \lambda_1^{(1)} x + g_{13} \sinh \lambda_2^{(1)} x + g_{14} \cosh \lambda_2^{(1)} x \tag{74}$$

with;

$$g_1 = \{g_{11},\ g_{12},\ g_{13}, g_{14}\}$$

For the ith Timochenko shaft segment, we get:

$$\bar{u}_i(x) = \left[\sin \lambda_1^{(i)} x \quad \cos \lambda_1^{(i)} x \quad \sinh \lambda_2^{(i)} x \quad \cosh \lambda_2^{(i)} x\right] \{g_i\} \tag{75}$$

with;

$$\{g_i\} = \left[g_{i1},\ g_{i2},\ g_{i3}, g_{i4}\right]^T$$

Using Equation (64), we obtain the following relationships related to the rest of the shaft segments:

$$\begin{aligned} & g_2 = B_1\ \mathrm{g}_1, \\ & g_3 = B_2\ \mathrm{g}_2 = B_2\ B_1\ \mathrm{g}_1 \\ & \vdots \\ & g_n = B_{n-1}\ \mathrm{g}_{n-1} = B_{n-1}\ B_{n-2} ... B_3\ B_2\ B_1\ \mathrm{g}_1 \end{aligned} \tag{76}$$

Description of the Analyzed System

In order to validate the proposed technique, consider a numerical example from ref. [16] involving a nonuniform (two-step) Timoshenko shaft composed of six segments each with a length of $L_i = 0.20\ m$, and diameter $d_i^{(s)} = 0.03\ m$ or $0.04\ m$, carrying three identical rigid disks as depicted in Figure 5. Each disk

has a thickness of $h = 0.004\ m$ and diameter of $d^{(d)} = 0.36\ m$. The material properties for the shaft are Young's modulus, $E = 2.068\ (10^{11})\ N/m^2$, shear coefficient, $\bar{k} = 0.75$, and shear modulus, $G = 0.795\ (10^{11}) N/m^2$. The mass density for the disk (or shaft) material is $\rho_i^{(d)} = \rho_i^{(s)} = 7850\ kg/m^3$.

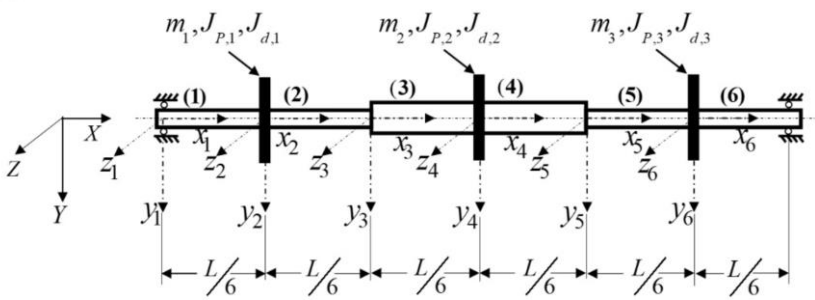

Figure 5: A nonuniform (two-step) Timoshenko shaft carrying three identical rigid disks

The eigenvalue Equation (72) is solved using a developed program in Fortran 90 language. The lowest five natural frequencies ω_s $(s = 1,2,...,5)$ obtained from the presented method and those obtained using FEM in [16] are listed in Table 1.

Table 1: Comparison of the lowest five natural frequencies $\omega_1 - \omega_5$ (with $\Omega = 0$)

Mode	**Natural frequencies** ω_s $(s = 1,2,...,5)$**, with** $\Omega = 0$ (rad/s)	
	Present Study	FEM in Ref. [16]
1^{st}	140.72011	140.7202
2^{nd}	434.46529	434.4659
3^{rd}	925.09181	925.0961
4^{th}	1490.61536	1490.6195
5^{th}	1697.21160	1697.2179

Table 1 shows that the lowest five natural frequencies obtained from the presented approach agree perfectly with those obtained from the conventional FEM in [16]. Associated natural mode shapes are depicted in Figures 6-10. It is to be noted that the vibration Equations (8a) and (9a) do not contain any term likely to limit the amplitudes of free vibrations. For that, all obtained mode

shapes are normalized such that the maximum value of each mode is equal to unity.

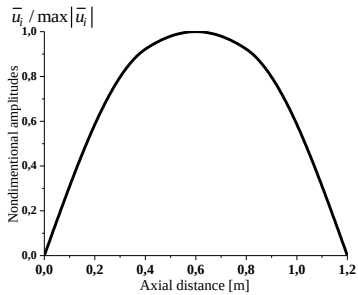

Figure 6: The first natural mode shape of transverse vibrations

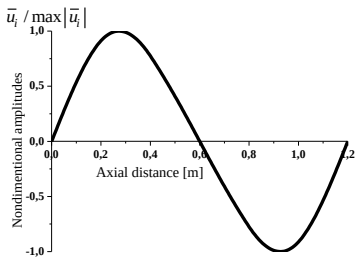

Figure 7: The second natural mode the shape of transverse vibrations

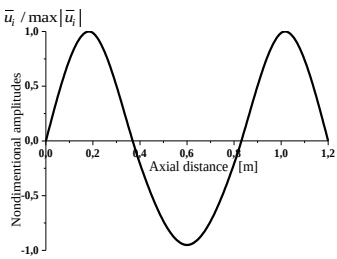

Figure 8: The third natural mode shape of transverse vibrations

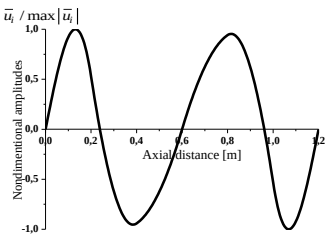

Figure 9: The fourth natural mode the shape of transverse vibrations

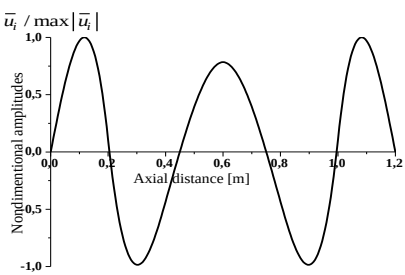

Figure 10: The fifth natural mode shape of transverse vibrations

Table 2 lists the lowest five forward and backward whirling speeds $\tilde{\omega}_s^F$ and $\tilde{\omega}_s^B$ $(s=1,2,...,5)$, taking into account the gyroscopic moment of the shaft,

obtained from the presented approach and those obtained using FEM and another analytical method in [16].

From Table 2, it is seen that all values of forwarding and backward whirling speeds with the gyroscopic moment of the shaft considered, obtained from this article are in remarkably good agreement with those obtained from ref. [16] using the conventional FEM and another analytical method.

Table 3 shows a comparison between the lowest five forward and backward whirling speeds $\widetilde{\omega}_s^F$ and $\widetilde{\omega}_s^B$ $(s=1,2,...,5)$ of the analyzed system with gyroscopic moment of the shaft neglected, obtained from the presented approach and those obtained using FEM and another analytical method in ref. [16].

Table 2: Comparison of the lowest five forward and backward whirling speeds, with gyroscopic moment of the shaft considered

Whirling speeds $\widetilde{\omega}_s$ with $\Omega = \widetilde{\omega}_s$ (rad/s)				
Direction of whirl		**Present Study**	**FEM in Ref [16]**	**Analytical method in Ref [16]**
Forward	$\widetilde{\omega}_1^F$	147.06340	147.0635	147.0635
	$\widetilde{\omega}_2^F$	480.87540	480.8764	480.8763
	$\widetilde{\omega}_3^F$	932.46869	932.4732	932.4729
	$\widetilde{\omega}_4^F$	5355.19469	5355.6869	5355.2862
	$\widetilde{\omega}_5^F$	6216.88169	6217.4720	6216.9834
Backward	$\widetilde{\omega}_1^B$	134.99264	134.9927	134.9927
	$\widetilde{\omega}_2^B$	391.214530	391.2148	391.2148
	$\widetilde{\omega}_3^B$	896.275739	896.2792	896.2790
	$\widetilde{\omega}_4^B$	960.383015	960.3859	960.3858
	$\widetilde{\omega}_5^B$	1068.337680	1068.3425	1068.3423

It should be noticed that in [16], the value of the fourth forward whirling speed, $\widetilde{\omega}_4^F$ obtained using an analytical method is not closed to that calculated using FEM from the same reference. From Table 3, it is seen that all values of forwarding and backward whirling speeds obtained by means of the presented approach, with gyroscopic moment of the shaft neglected, are in remarkably good agreement with the corresponding ones obtained using the conventional FEM in ref. [16]. Figure 11 represents the mode shapes obtained from existing literature, (Figure 14 in ref [16]).

Table 3: Comparison of the lowest five forward and backward whirling speeds, with gyroscopic moment of the shaft neglected

Whirling speeds $\tilde{\omega}_s$ with $\Omega = \tilde{\omega}_s$ (*rad / s*)				
Direction of whirl		**Present Study**	**FEM in Ref [16]**	**Analytical method in Ref [16]**
Forward	$\tilde{\omega}_1^F$	147.05248	147.0526	147.0526
	$\tilde{\omega}_2^F$	480.64971	480.6507	480.6506
	$\tilde{\omega}_3^F$	932.01115	932.0156	896.2792
	$\tilde{\omega}_4^F$	5320.47043	5320.9487	960.3859
	$\tilde{\omega}_5^F$	6172.09668	6172.6673	6172.1948
Backward	$\tilde{\omega}_1^B$	135.00107	135.0011	135.0011
	$\tilde{\omega}_2^B$	391.34774	391.3481	391.3480
	$\tilde{\omega}_3^B$	896.60700	896.6104	896.6103
	$\tilde{\omega}_4^B$	960.55576	960.5586	960.5585
	$\tilde{\omega}_5^B$	1068.64318	1068.6480	1068.6478

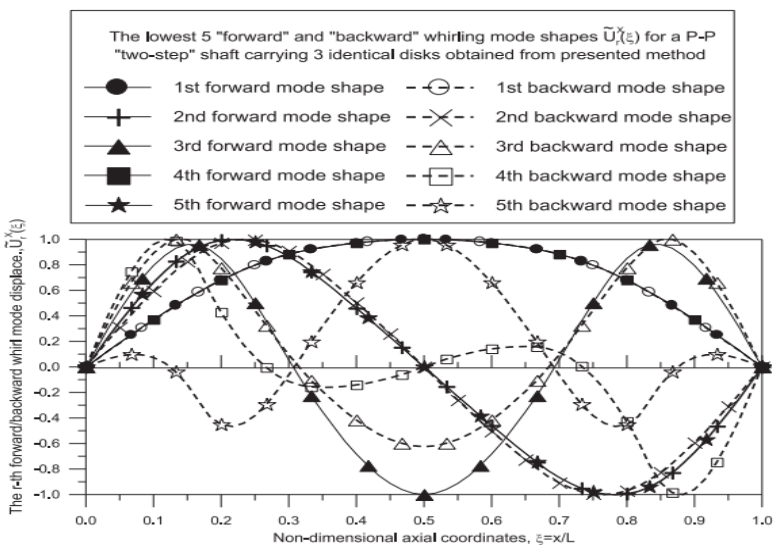

Figure 11: The five lowest whirling mode shapes obtained by Wu et al. (Figure 14 in ref. [16])

Figure 11 is imported from the reference ([16], Figure 14]). It represents the lowest five forward and backward whirling mode shapes obtained using an analytical method, represented by solid lines (—) and dotted lines (... ...), respectively. It is seen that the fourth and first forward mode shapes, denoted by solid squares (-■-) and solid circles (-●-), respectively, coincide. The same finding is noted concerning the fifth and second forward mode shapes, denoted by solid stars (-★-) and solid triangles (-▲-), respectively. This allows concluding that the fourth and fifth forward mode shapes are not plotted carefully in [16], because according to the vibration theory, they should contain three nodes, and four nodes, respectively.

The obtained lowest five forward and backward whirling mode shapes using the presented approach are depicted in Figures 12-16.

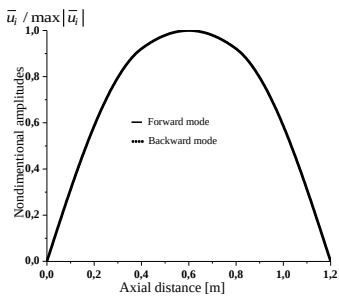

Figure 12: The first whirling mode shape

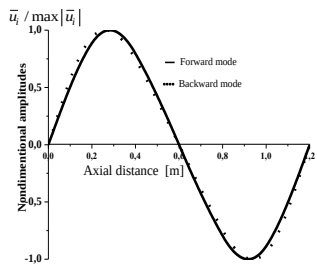

Figure 13: The second whirling mode shape

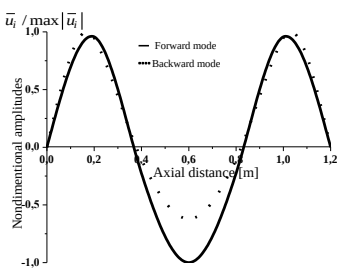

Figure 14: The third whirling mode shape

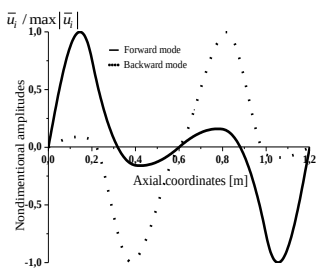

Figure 15: The fourth whirling mode shape

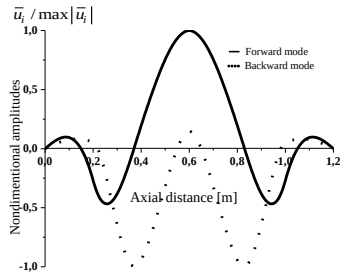

Figure 16: The fifth whirling mode shape

The first mode shapes of the analyzed system for forward and backward whirls plotted in Figure 12 are overlapped and also identical to the first natural mode shape in Figure 6. This is because the corresponding first forward and backward whirling speeds $\widetilde{\omega}_1^F = 147.05248\, rad/s$ and $\widetilde{\omega}_1^B = 135.00107\, rad/s$ do not differ too much from the first natural frequency $\omega_1 = 140.72011\, rad/s$. The distinction between the whirling mode shapes becomes obvious from the second one. The gyroscopic moment of the shaft increases the forward whirling speeds and reduces the backward ones. This phenomenon is understood as the stiffening and softening of the gyroscopic effect. It is noted that the configuration of all mode shapes is symmetrical due to the assumption that the analyzed shaft-disks system resting on identical bearings has symmetric properties in stiffness and inertia.

Conclusion

In this work, whirling vibrations of a Timoshenko type shaft with two steps, carrying three identical rigid disks are investigated using an analytical approach based on relationships between the vectors of solution coefficients. The developed relationships in this work allow an analysis of the effects of rotary inertia, shear deformation, and gyroscopic moments on the dynamic behavior of the Timohenko shaft-disk system. The computed natural frequencies and critical (forward and backward) whirling speeds proved to coincide with those obtained using conventional FEM from the available literature (ref. [16]). The obtained numerical results indicate that the analytical approach developed in this article provides an accurate calculation of eigenquantities such as whirling speeds and mode shapes of rotating stepped Timoshenko shaft carrying multiple disks. The given relationships in this work can easily take into account a transverse crack and linear model of damping and are well-suited to extend to the study of a multi-disk rotor with any number of steps on flexible bearing supports.

Nomenclature

E_i, G_i Young's modulus and shear modulus of the *i*th shaft segment $\left[N/m^2\right]$

$I_{y,i} = I_{z,i} = I_i$ diametric moment of inertia of the cross-sectional area S_i of the *i*th shaft segment about the y- or z-axis

$I_{p,i}$ polar moment of inertia of the cross-sectional area S_i of the *i*th shaft segment

$J_{d,i}, J_{P,i}$ diametric moment of inertia and polar moment of inertia of the *i*th rigid disk $\left[kgm^2\right]$

$\overline{k}_i$ shear correction factor for the *i*th shaft segment

L_i lenght of the *i*th shaft segment $\left[m\right]$

m_i mass of the *i*th rigid disk (*i*), located at the end of the *i*th shaft segment $\left[kg\right]$

S_i cross-sectional area of the *i*th shaft segment $\left[m^2\right]$

$\overline{u}_{y,i}(x)$, $\overline{u}_{z,i}(x)$ deflection amplitude of the cross-sectional centroid of the *i*th shaft segment, at axial coordinate *x*, in the vertical and horizontal directions, respectively $\left[m\right]$

$u_i(x,t) = u_{y,i}(x,t) + ju_{z,i}(x,t)$ complex variable representation of rotor deflection

$\frac{\partial \overline{u}_{z,i}(x)}{\partial x}, \frac{\partial \overline{u}_{y,i}(x)}{\partial x}$ slope amplitude of the elastic axis of the *i*th shaft segment at axial coordinate *x*, in the $x_i y_i$ and $x_i z_i$ planes, respectively $\left[rad\right]$

$\overline{\gamma}_{xy,i}(x), \overline{\gamma}_{xz,i}(x)$ amplitudes of transverse shear angles of the *i*th shaft cross section at axial coordinate *x*, in the $x_i y_i$ and $x_i z_i$ planes, respectively $\left[rad\right]$

$\gamma_i(x,t) = \gamma_{xy,i}(x,t) + j\gamma_{xz,i}(x,t)$ complex variable representation of the shear angle

ρ_i mass density of the *i*th shaft segment $\left[kg/m^3\right]$

$\widetilde{\omega}_s$ whirling speed $\left[rad/s\right]$

ω natural frequency $\left[rad/s\right]$

Ω rotor speed $\left[rad/s\right]$

$\overline{\psi}_{z,i}(x)$, $\overline{\psi}_{y,i}(x)$ slope amplitude due to bending of the *i*th shaft cross section at axial coordinate *x*, in the $x_i y_i$ and $x_i z_i$ planes, respectively $\left[rad\right]$

$\psi_i(x,t) = \psi_{z,i}(x,t) - j\psi_{y,i}(x,t)$, complex variable representation of slope due to bending

References

[1] M. J. Legaz, S. Amat, and S. Busquier, "Marine Propulsion Shafting: A Study of Whirling Vibrations," *J. Sh. Res.*, vol. 65, no. 01, pp. 55–61, Mar. 2021, doi: 10.5957/JOSR.05180022.

[2] M. Klannerk, M. S. Prem, and K. Ellermann, "Quasi-Analytical Solutions for The Whirling Motion of Multi-Stepped Rotors with Arbitrarily Distributed Mass Unbalance Running in Anisotropic Linear Bearings," *Bull. Polish Acad. Sci. Tech. Sci.*, vol. 69, no. 6, 2021, doi:

10.24425/BPASTS.2021.138999.

[3] R. L. Eshleman and R. A. Eubanks, "On the Critical Speeds of a Continuous Rotor," *J. Eng. Ind.*, vol. 91, no. 4, pp. 1180–1188, Nov. 1969, doi: 10.1115/1.3591768.

[4] A. Bose and P. Sathujoda, "Free Vibration Analysis of an Exponentially Graded Shaft System Subjected to Thermal Gradients," *AIP Conf. Proc.*, vol. 2341, no. 1, p. 020009, May 2021, doi: 10.1063/5.0049908.

[5] G. Curti, F. A. Raffa, and F. Vatta, "An Analytical Approach to the Dynamics of Rotating Shafts," *Mecc. 1992 274*, vol. 27, no. 4, pp. 285–292, Dec. 1992, doi: 10.1007/BF00424368.

[6] J. W. Z. Zu and R. P. S. Han, "Natural Frequencies and Normal Modes of a Spinning Timoshenko Beam With General Boundary Conditions," *J. Appl. Mech.*, vol. 59, no. 2S, pp. S197–S204, Jun. 1992, doi: 10.1115/1.2899488.

[7] R. P. S. Han and J. W. Z. Zu, "Analytical Dynamics of a Spinning Timoshenko Beam Subjected to a Moving Load," *J. Franklin Inst.*, vol. 330, no. 1, pp. 113–129, Jan. 1993, doi: 10.1016/0016-0032(93)90024-O.

[8] F. A. Raffa and F. Vatta, "Gyroscopic Effects Analysis in the Lagrangian Formulation of Rotating Beams," *Mecc. 1999 345*, vol. 34, no. 5, pp. 357–366, 1999, doi: 10.1023/A:1004781602416.

[9] F. A. Raffa and F. Vatta, "Equations of Motion of an Asymmetric Timoshenko Shaft," *Mecc. 2001 362*, vol. 36, no. 2, pp. 201–211, 2001, doi: 10.1023/A:1013079613566.

[10] S. C. Hsieh, J. H. Chen, and A. C. Lee, "A Modified Transfer Matrix Method for the Coupling Lateral and Torsional Vibrations of Symmetric Rotor-Bearing Systems," *J. Sound Vib.*, vol. 289, no. 1–2, pp. 294–333, Jan. 2006, doi: 10.1016/J.JSV.2005.02.004.

[11] T. N. Shiau, E. C. Chen, K. H. Huang, and W. C. Hsu, "Dynamic Response of a Spinning Timoshenko Beam with General Boundary Conditions under a Moving Skew Force Using Global Assumed Mode Method," *JSME Int. J. Ser. C Mech. Syst. Mach. Elem. Manuf.*, vol. 49, no. 2, pp. 401–410, Dec. 2006, doi: 10.1299/JSMEC.49.401.

[12] K. Torabi and H. Afshari, "Exact Solution for Whirling Analysis of Axial-Loaded Timoshenko Rotor Using Basic Functions," *Eng. Solid Mech.*, vol. 4, pp. 97–108, 2016, doi: 10.5267/j.esm.2015.11.001.

[13] H. Afshari and M. Irani Rahaghi, "Whirling Analysis of Multi-Span Multi-Stepped Rotating Shafts," *J. Brazilian Soc. Mech. Sci. Eng. 2018 409*, vol. 40, no. 9, pp. 1–17, Aug. 2018, doi: 10.1007/S40430-018-1351-X.

[14] Y. Zhang, X. Yang, and W. Zhang, "Modeling and Stability Analysis of a Flexible Rotor Based on the Timoshenko Beam Theory," *Acta Mech. Solida Sin. 2019 333*, vol. 33, no. 3, pp. 281–293, Oct. 2019, doi: 10.1007/S10338-019-00146-Y.

[15] H. Afshari, K. Torabi, and A. Jafarzadeh Jazi, "Exact Closed Form

Solution for Whirling Analysis of Timoshenko Rotors with Multiple Concentrated Masses," *https://doi.org/10.1080/15397734.2020.1737112*, vol. 50, no. 3, pp. 969–992, 2020, doi: 10.1080/15397734.2020.1737112.

[16] J. S. Wu and T. F. Hsu, "An Efficient Approach for Whirling Speeds and Mode Shapes of Uniform and Nonuniform Timoshenko Shafts Mounted by Arbitrary Rigid Disks," *Eng. Reports*, vol. 2, no. 7, p. e12183, Jul. 2020, doi: 10.1002/eng2.12183.

[17] J. Kolenda, "Forced Vibrations of Shaft Line Taking in to Account The Flexural Stiffness Asymmetry And Foundation Flexibility," *J. Theor. Appl. Mech.*, vol. 16, no. 4, pp. 517–535, 1978.

[18] J. Kolenda, "A More Precise Description of Shaft Line Vibrations," *J. Theor. Appl. Mech.*, vol. 17, no. 2, pp. 105–126, 1979.

[19] Z. H. Cherif and C. Kandouci, "Dynamic Characteristics of Multi-Disk Shaft System using the Vectors of Solution Coefficients," *J. Mech. Eng.*, vol. 17, no. 3, pp. 95–115, 2020.

[20] K. Chahr-Eddine and A. Yassine, "Forced Axial and Torsional Vibrations of a Shaft Line Using the Transfer Matrix Method Related to Solution Coefficients," *J. Mar. Sci. Appl. 2014 132*, vol. 13, no. 2, pp. 200–205, May 2014, doi: 10.1007/S11804-014-1251-0.

[21] P. Natanson, *Short Course in Higher Mathematics*. Publ. Lan. (St. Petersburg), pp. 399-401, 1999.

[22] Giancarlo Genta, *Dynamics of Rotating Systems*. Berlin: Springer Science and Business Media, pp. 215-216, 2005.

[23] J. S. Wu, *Analytical and Numerical Methods for Vibration Analyses*. John Wiley & Sons Singapore Pte. Ltd., pp.680, 2015.